Journal of Control, Automation and Electrical Systems (2020) 31:494–510
https://doi.org/10.1007/s40313-020-00573-0

Distribution System Planning with Representation of Uncertainties Based on Interval Analysis

Felipe da S. Seta[1] · **Leonardo W. de Oliveira**[2] · **Edimar J. de Oliveira**[2]

Received: 10 May 2019 / Revised: 9 January 2020 / Accepted: 22 January 2020 / Published online: 6 February 2020

Abstract
This work presents an approach for optimal distribution system planning (DSP) to minimize the total costs of expansion and operation with the representation of uncertainties in the load demand and in the wind-based distributed generation (WDG). The proposed approach, called interval distribution system planning (I-DSP), is based on an interval power flow (IPF) and the metaheuristic artificial immune system (AIS). The IPF is used to obtain an interval of the total cost that reflects the uncertainties over load and generation. The interval cost is the merit function of the optimization algorithm. The network constraints as the limits of current, voltage and power from substations, in addition to the radiality and connectivity are taken into account. Well-known test systems are used to assess the impact of the uncertainties representation in the DSP problem.

Keywords Artificial immune system · Distribution system planning · Interval mathematics · Optimization · Uncertainties · Wind-distributed generation

List of Symbols

Sets and Indexes

a	Index for cable type
e	Index for existing cable type
d	Index for deterministic variables
i	Index for interval variables
f	Index for system buses
j	Index for buses directly connected to f
fj	Index for system branches
n	Index for substations
lo, up	Index for lower and upper limits for any variable
NBP	Set of candidate branches
NC	Set of cable types
NBE	Set of existing branches
NDG	Set of buses candidate for receiving WDG
NSP	Set of proposed substations, i.e., substations candidate for building
NSE	Set of existing substations
NST	Set of existing and candidate substations
NBT	Set of existing and candidate branches
NBU	Set of buses
Ω_f	Set of buses directly connected to f
P	Set of initial candidate solutions

Parameters

CI_a	Cost for building a new branch with cable type 'a' (US$/km)
CR_{ea}	Cost for retrofitting an existing branch of cable type 'e' by replacing it by cable type 'a' (US$/km)
CWT_f	Cost for installation of wind turbine at bus f (US$)
CB_n	Cost for building a proposed substation 'n' (US$)

✉ Felipe da S. Seta
felipe.seta@cefet-rj.br

[1] Department of Electrical Engineering, Federal Center of Technological Education "Celso Suckow da Fonseca", Angra dos Reis, RJ, Brazil

[2] Department of Electrical Engineering, Federal University at Juiz de Fora (UFJF), Juiz de Fora, MG, Brazil

CE_n	Cost for expanding the capacity of an existing substation (US$)
C_{op}	Substation operation cost (US$/kVA^2 h)
C_l	Energy loss cost (US$/kWh)
C_{wg}	Operating and maintenance cost of the wind turbine (US$/kWh)
C_{pe}	Energy purchase cost (US$/kWh)
l_{fj}	Length of branch *fj* (km)
VP	Conversion of any cost to its present value
g_{fj}	Conductance of branch *fj*
α	Number of hours in 1 year
φ_S, φ_l	Loss factors for substations and branches
τ	Annual interest rate
T	Planning horizon in years
Pd_f^i, Qd_f^i	Interval active and reactive loads
Pd_f^d, Qd_f^d	Deterministic active and reactive loads
α_{pkl}, α_{pku}, α_{qkl}, α_{qku}	Active and reactive load percent variations
Pwt_f^{lo}, Pwt_f^{up}	Limits of the active power from a wind generator
Qwt_f^{lo}, Qwt_f^{up}	Limits of the reactive power from a wind generator
V_f^{lo}, V_f^{up}	Limits for the interval voltage variable
I_{fj}^{lo}, I_{fj}^{up}	Limits of the interval current variable
Ss_n^{lo}, Ss_n^{up}	Limits of the apparent power supplied by substation
V^{min}, V^{max}	Minimum and maximum operational voltage levels
I_{fj}^{max}	Maximum current at branch *fj*
Ss_n^0	Maximum apparent power from existing substation
Ss_n^{EX}	Predefined value of apparent power considered as an expansion for existing substation
Ss_n^{NS}	Maximum apparent power from new substation
v^{lo}, v^{up}	Wind speed limits
α_{wl}, α_{wu}	Percent variations of the wind speed
v_{in}, v_n, v_{ou}	Input, nominal and output speeds of a wind generator
P_n	Nominal WDG active power
ap, bp	Coefficients that relate wind speed to the active power from a wind generator
cq, dq	Coefficients that relate wind speed to the reactive power from a wind generator
X_p, Y_p, Z_p, W_p	Rows of the inverse Jacobian matrix at the solution point of deterministic power flow
Jac^i, Jac^d	Interval and deterministic Jacobian matrix
C	Preconditioning matrix given by the inverse of the Jacobian matrix at the solution point of deterministic power flow
Id	Identity matrix
m_x, r_X	Midpoint and radius of interval $X=[x_1; x_2]$
$round(.)$	Rounding operator
β	Cloning parameter of the CLONR algorithm
nb	Number of candidate solutions for cloning
db	Number of candidate solutions randomly generated for the receptor editing process
$f^*(i)$	Normalized fitness of a candidate solution i
$f(i)$	Midpoint fitness of a candidate solution i
f_{av}	Average fitness for clone set of CLONR
$\delta*$	Standard deviation
$p(ic)$	Probability of clone ic to be mutated ($p(ic)\in[0,1]$)
h	Mutation parameter of the CLONR algorithm
h_1, h_2	Low- and high-mutation parameters of the CLONR algorithm
Nab	Number of candidate solutions (antibodies) of set P
Nab_dist	Number of unique individuals of the CLONR algorithm
$gmax$	Maximum number of I-DSP algorithm iterations
$gest$	Number of iterations in which the best solution of P remains unchanged

$gimp$ Number of iterations in which the process stagnates

div, $limd$ Solutions diversity and its inferior limit

δ_S, δ_l, δ_{wt}, δ_{pe} Auxiliary variables for the calculation of the following interval costs: operating of the substations, energy loss, wind power generation and the energy purchase cost, respectively

ε_{vo}, ε_{cu}, ε_{ap}, ε_{acp}, ε_{lo}, ε_{op}, ε_{pe}, ε_{tc} Maximum relative percent errors between IPF and MCS for voltages, currents, apparent power from substation, active power from substation, loss cost, operational cost, energy purchase cost and total cost, respectively

Variables

$x_{fj,a}^{bc}$ Binary variable associated with building branch fj with cable type 'a'

$x_{fj,a}^{br}$ Binary variable associated with retrofitting branch fj

x_f^{wt} Binary variable associated with retrofitting branch fj

x_n^{sc} Binary variable associated with building the proposed substation

x_n^{sr} Binary variable associated with expanding the existing substation

x_n^{oc} Binary variable associated with operating substation

x_{fj}^{cc} Binary variable associated with building branch fj

v^i, v^d Interval and deterministic wind speed

Ss_n^i Apparent power supplied by substation 'n'

L_{fj}^i, L_{fj}^d Interval and deterministic power loss of branch fj

Pwt_f^i, Qwt_f^i Active and reactive power from wind generator at bus f

Ps_n^i Active power supplied by substation n

ΔL_{fj}^i Power loss increment of branch fj

V_f^i Interval voltage magnitude at bus f

V_f^d, V_j^d Deterministic voltage magnitude at bus f and j

I_{fj}^i Interval current magnitude at branch fj

θ_{fj}^d Deterministic phase angle between buses f and j

θ_f^d Deterministic phase angle at bus f

Ps_f^i, Qs_f^i Interval active and reactive powers supplied by substation at bus f

P_{fj}^i, Q_{fj}^i Interval active and reactive power flows at branch fj

P_f^i, Q_f^i Interval active and reactive powers injected at bus f

ΔP_f^i, ΔQ_f^i Interval active and reactive power mismatches at bus f

$\Delta\theta^i$, ΔV^i Interval increments of phase angle and voltage magnitude

θ_f^i Interval phase angle at bus f

X^h Interval solution vector of the IPF updated at each iteration h

x^h Vector given by the midpoints of the intervals contained in X^h

x, $f(x)$ State and power mismatch vectors, respectively

$K(x^h,X^h)$, $h(x^h)$ Krawczyk operator and iteration counter

ε^i Pre-specified tolerance used as IPF convergence criterion

OV^i, OV^d, ΔOV^i Interval, deterministic and interval increment for any output variable

μ Measure function used for comparing intervals

$Nc(i)$ Number of clones for a selected candidate solution i

1 Introduction

The DSP becomes a problem with many challenges as the rate of load growth increases and operational reach dangerous limits. In this way, investments in the expansion and operation of electrical networks must be made by distribution companies to ensure the quality and reliability of the energy supply (Mazhari et al. 2016; Junior et al. 2014).

Among the strategies for the expansion of electrical distribution systems (EDS), the most traditional actions include: expansion and retrofitting of branches, construction and reinforcement of substations and network reconfiguration (Mazhari et al. 2016; Junior et al. 2014; Naderi et al. 2012; Porkar et al. 2010; Alishahi et al. 2012; Bin Humayd and Bhattacharya 2017; Vélez et al. 2014; Sahoo and Ganguly 2011; Ravadanegh et al. 2016; Oliveira et al. 2016; Lavorato et al. 2010; Nahman and Peric 2008). These actions aim to minimize investment and operational costs.

Uncertainties over loads, mainly due to forecast and measurement errors, impact the decisions on the planning options (Oliveira et al. 2016; Zhang et al. 2012). Recently, the wind-based DG has been included in the planning of distribution systems, since modern distribution networks have included heterogeneous distributed resources (Ortiz et al. 2019; Ehsan et al. 2019; Zhang et al. 2018). The uncertainty over renewable wind-based DG due to intermittency of primary sources (Naderi et al. 2012; Porkar et al. 2010; Alishahi et al. 2012; Oliveira et al. 2016; Borges and Martins 2012) requires techniques that can adequately and efficiently model the impact of these uncertainties (Naderi et al. 2012; Porkar et al. 2010; Alishahi et al. 2012; Bin Humayd and Bhattacharya 2017). Therefore, the representation of uncertainties is extremely important for the DSP and gives it more realism. In Ravadanegh et al. (2016), the load uncertainty is represented by the point estimate approach and binary global search optimization is proposed to solve the DSP problem. The theory of multiple scenarios is a strategy widely used in the literature for modeling uncertainties and is applied in Borges and Martins (2012), Asensio et al. (2018), Ahmadigorji et al. (2018), Amjady et al. (2018) and Ortiz et al. (2018) to handle uncertainties over load and DG for planning EDS. In Asensio et al. (2018) and Ortiz et al. (2018), a stochastic scenario-based programming is used, whereas the theory of multiple scenarios is associated with information-gap decision theory in Ahmadigorji et al. (2018).

Uncertainties can also be represented by using fundamentals of interval mathematics (Oliveira et al. 2016; Pereira et al. 2012; Wang and Alvarado 1992; Chaturvedi et al. 2006; Saric and Stankovic 2006), where load and wind speed are not given by single points, but they can vary within known ranges. An interval analysis for a multiobjective reconfiguration to minimize technical losses and improve reliability is proposed in Zhang et al. (2012). In Oliveira et al. (2016), interval mathematics is used for EDS reconfiguration to minimize energy losses with uncertainties over load and wind-based DG. Qiao et al. (2017) propose a comprehensive system model of a natural gas and electricity coupled network, where the impact of the active power output uncertainty of wind farms was studied, and the interval flow of the natural gas system was analyzed by two proposed methods. An interval estimation of voltage magnitude in radial distribution feeder with minimal data acquisition requirements is made in Rasmussen et al. (2019).

Modeling and solving the DSP is a complex task because it is a nonlinear mixed integer and combinatorial problem that has non-convex search space (Mazhari et al. 2016; Junior et al. 2014; Naderi et al. 2012; Porkar et al. 2010; Alishahi et al. 2012; Bin Humayd and Bhattacharya 2017; Vélez et al. 2014; Sahoo and Ganguly 2011; Ravadanegh et al. 2016; Oliveira et al. 2016; Lavorato et al. 2010; Nahman and Peric 2008; Zhang et al. 2012; Borges and Martins 2012). In addition, the radial and connectivity constraints make this problem even more difficult to be solved. The evaluation of all possible combinations allows finding the global optimal solution, but it is computationally unsuitable for the EDS requirements. From such aspects, metaheuristics can be applied to the DSP because they can efficiently sweep huge search space, as it is done in several works (Mazhari et al. 2016; Junior et al. 2014; Naderi et al. 2012; Vélez et al. 2014; Sahoo and Ganguly 2011; Oliveira et al. 2016; Lavorato et al. 2010; Nahman and Peric 2008; Zhang et al. 2012; Borges and Martins 2012).

In this way, the present work proposes an approach, based on IPF and the metaheuristic artificial immune system (AIS) (Oliveira et al. 2014, 2016), that considers uncertainties over the load demand and the wind-based DG through an IPF to solve the DSP problem. Although the DSP is static, a long-term planning is performed through the decision taking for the operation horizon made in a unique stage, but with the present values of the related costs. The proposed I-DSP approach considers the expansion and/or construction of new substations, installation of new primary feeders and/or reinforcement of the existing ones, installation of wind-based DG and network reconfiguration. The objective is to minimize the investment in substations, branches and wind-based DG, the energy purchase costs, as well as the operational costs related to energy losses, substations and wind power generation. The input random variables are the loads and wind speed; as a consequence, the uncertainties are propagated to the output power flow variables and total cost that are given in interval form (Oliveira et al. 2016; Pereira et al. 2012). A methodology for comparing intervals (Alolyan 2011) is used to determine the best option. Network limits and constraints are incorporated into the model, where a radial and connected system is ensured by using graph theory and the AIS mechanisms. The main contributions of this paper are:

- a novel application of interval mathematics for assessing the impact of representing uncertainties in the DSP with DG;
- an optimization algorithm proper to model uncertainties in power systems planning for random parameters having large variations, which maintains the power flow variables within suitable values;

- the development of a novel optimization algorithm involving the AIS technique with the IPF embedded untapped for the DSP problem.

2 I-DSP Model

The I-DSP problem is modeled in this section. The objective function (*OBF*) is formulated as:

$$\begin{aligned} Min\ OBF = & \sum_{fj\in NBP}\sum_{a\in NC}\left(CI_a\cdot l_{fj}\cdot x_{fj,a}^{bc}\right)+\sum_{fj\in NBE}\sum_{\substack{a\in NC\\ a\neq e}}\left(CR_{ea}\cdot l_{fj}\cdot x_{fj,a}^{br}\right)\\ & +\sum_{f\in NDG}\left(CWT_f\cdot x_f^{wt}\right)+\sum_{n\in NSP}\left(CB_n\cdot x_n^{sc}\right)+\sum_{n\in NSE}\left(CE_n\cdot x_n^{sr}\right)\\ & +VP\cdot\delta_{\mathrm{S}}\cdot\sum_{n\in NST}\left(Ss_n^i\right)^2\cdot x_n^{oc}+VP\cdot\delta_{\mathrm{l}}\cdot\sum_{fj\in NBT}\left(L_{fj}^i\cdot x_{fj}^{cc}\right)\\ & +VP\cdot\delta_{\mathrm{wt}}\cdot\sum_{f\in NDG}\left(Pwt_f^i\right)\cdot x_f^{wt}+VP\cdot\delta_{\mathrm{pe}}\cdot\sum_{n\in NST}\left(Ps_n^i\right)\cdot x_n^{oc}. \end{aligned} \tag{1}$$

The total cost of investment, operation and energy purchase in market related to an EDS, considering the expansion options of the present work, is modeled in the *OBF* in (1). The first five terms refer to the investments in building new branches, replacing existing branches, installing wind-based DG, building new substations and expanding the existing ones, respectively. These costs are given by deterministic values, and they are functions of the binary optimization decision variables: $x_{fj,a}^{bc}, x_{fj,a}^{br}, x_f^{wt}, x_n^{sc}$ and x_n^{sr}. The sixth term is the present value of the interval operating cost of the substations in function of their interval apparent powers. The seventh and eighth terms give the interval operating costs of the energy loss and wind power generation, respectively, in their present values. The ninth term, in turn, establishes the present value of the interval energy purchase cost, which depends on the interval active powers from the substations. Therefore, the *OBF* is represented in interval form due to the last four terms in (1). The power loss of branch *fj* is an interval output variable that is formulated as in (2) and (3).

$$L_{fj}^i = L_{fj}^d + \Delta L_{fj}^i, \tag{2}$$

$$L_{fj}^d = g_{fj}\cdot\left[\left(V_f^d\right)^2+\left(V_j^d\right)^2-2\cdot V_f^d\cdot V_j^d\cdot\cos\left(\theta_{fj}^d\right)\right]. \tag{3}$$

The variables δ_{S}, δ_{l}, δ_{wt} and δ_{pe} are obtained from (4) to (7), whereas the factor to convert any cost to its present value is given by (8).

$$\delta_{\mathrm{S}} = \alpha\cdot\varphi_S\cdot C_{\mathrm{op}}, \tag{4}$$

$$\delta_{\mathrm{l}} = \alpha\cdot\varphi_l\cdot C_{\mathrm{l}}, \tag{5}$$

$$\delta_{\mathrm{wt}} = \alpha\cdot C_{wg}, \tag{6}$$

$$\delta_{\mathrm{pe}} = \alpha\cdot C_{\mathrm{pe}}, \tag{7}$$

$$VP = \frac{(1+\tau)^T-1}{\tau\cdot(1+\tau)^T}. \tag{8}$$

The proposed optimization model for the I-DSP problem is subjected to the constraints hereafter.

$$Ps_f^i + Pwt_f^i - Pd_f^i - \sum_{j\in\Omega_f} x_{fj}^{cc}\cdot P_{fj}^i = 0,\quad f\in NBU, \tag{9}$$

$$Qs_f^i + Qwt_f^i - Qd_f^i - \sum_{j\in\Omega_f} x_{fj}^{cc}\cdot Q_{fj}^i = 0,\quad f\in NBU, \tag{10}$$

$$Pd_f^i = \left[Pd_f^d\cdot\left(1-\alpha_{pkl}\right);Pd_f^d\cdot\left(1+\alpha_{pku}\right)\right], \tag{11}$$

$$Qd_f^i = \left[Qd_f^d\cdot\left(1-\alpha_{qkl}\right);Qd_f^d\cdot\left(1+\alpha_{qku}\right)\right], \tag{12}$$

$$Pwt_f^i = \left[Pwt_f^{\mathrm{lo}};Pwt_f^{\mathrm{up}}\right], \tag{13}$$

$$Qwt_f^i = \left[Qwt_f^{\mathrm{lo}};Qwt_f^{\mathrm{up}}\right], \tag{14}$$

$$V_f^i = \left[V_f^{\mathrm{lo}};V_f^{\mathrm{up}}\right], \tag{15}$$

$$I_{fj}^i = \left[I_{fj}^{\mathrm{lo}};I_{fj}^{\mathrm{up}}\right], \tag{16}$$

$$Ss_n^i = \left[Ss_n^{\mathrm{lo}};Ss_n^{\mathrm{up}}\right], \tag{17}$$

$$V_f^{\text{lo}} \geq V^{\min}; V_f^{\text{up}} \leq V^{\max}, \tag{18}$$

$$x_{fj}^{cc} \cdot I_{fj}^{i} \leq I_{fj}^{\max} \cdot x_{fj}^{cc}, \tag{19}$$

$$Ss_n^i \leq Ss_n^0 + x_n^{sr} \cdot Ss_n^{\text{EX}}, \tag{20}$$

$$x_n^{sc} \cdot Ss_n^i \leq x_n^{sc} \cdot Ss_n^{\text{NS}}, \tag{21}$$

$$\sum_{fj \in NBT} x_{fj}^{cc} = NBU - NST, \tag{22}$$

$$x_{fj,a}^{bc}, x_{fj,a}^{br}, x_f^{wt}, x_n^{sr}, x_n^{sc}, x_n^{oc}, x_{fj}^{cc} \in \{0,1\}. \tag{23}$$

The interval active and reactive power balance constraints for each bus f are given in (9) and (10), respectively. When bus f has no a wind-based DG, both Pwt_f^i and Qwt_f^i are equal to zero. Constraints in (11) and (12) model the interval loads at bus f in relation to the respective deterministic loads, whereas the interval wind generation is modeled in (13) and (14). The IPF variables have their limits defined in (15)–(17). The interval limits must observe equipment capacities and operational limits as formulated in (18)–(21). Note that the power from an existing substation is limited by its capacity as well as by the allowed expansion as in (20), whereas a new substation has its capacity given in (21). Constraint in (22) provides a necessary condition to generate radial solutions, but it does not guarantee connected solutions. Therefore, in addition to (22), a graph theory-based algorithm is used to ensure the connectivity of the candidate topologies. The discrete feature of the planning decision variables is defined in (23).

The uncertainty level in load demand is established by variations percent α_{pk} and α_{qk} according to (11) and (12). The Pwt_f^{lo}, Pwt_f^{up}, Qwt_f^{lo} and Qwt_f^{up} limits are calculated from the interval wind speed (v^i) given by (24) and should meet the capacity of the wind DG (Oliveira et al. 2016).

$$v^i = \left[v^{\text{lo}}; v^{\text{up}}\right] = \left[v^d \cdot \left(1 - \alpha_{wl}\right); v^d \cdot \left(1 + \alpha_{wu}\right)\right]. \tag{24}$$

The wind speed variation impacts on the active and reactive power from wind generators according to (25) and (26) (Oliveira et al. 2016).

$$Pwt_f^i = \left[Pwt_f^{\text{lo}}; Pwt_f^{\text{up}}\right] = ap\left[v^{\text{lo}}; v^{\text{up}}\right] + bp, \tag{25}$$

$$Qwt_f^i = \left[Qwt_f^{\text{lo}}; Qwt_f^{\text{up}}\right] = cq\left[v^{\text{lo}}; v^{\text{up}}\right] + dq. \tag{26}$$

The input interval variables Pwt_f^i and Qwt_f^i are determined by interval arithmetic operations from (25) to (26). Details about the interval arithmetic operations are given in Pereira et al. (2012). The coefficients ap, bp, cq and dq of (25) and (26) are obtained by using a polynomial regression technique (Valentine and Van Dine 1963) applied to sample data. For active power from DG, Pwt, the polynomial regression technique (Valentine and Van Dine 1963) is applied to find the first-degree function formulated in (27) (Oliveira et al. 2016).

$$Pwt(v) = \begin{Bmatrix} 0, & \text{if } v \leq v_{\text{in}} \text{ or } v \geq v_{\text{ou}} \\ P_{\text{n}} \frac{v - v_{\text{in}}}{v_{\text{n}} - v_{\text{in}}} = av + b, & \text{if } v_{\text{in}} \leq v \leq v_{\text{n}} \\ P_{\text{n}}, & \text{if } v_{\text{n}} < v < v_{\text{ou}} \end{Bmatrix}. \tag{27}$$

For reactive power, Qwt, the polynomial regression technique (Valentine and Van Dine 1963) is also applied to find a first-degree function, but in this case, Qwt depends on the active power and generator type, which can be conventional squirrel cage or double-fed generator. The power factor of a squirrel cage generator is variable, and Qwt can be obtained from sample data. The double-fed generator, in turn, has a control speed based on the adjustment of the rotor voltage and currents that allows an operation with a constant power factor (Oliveira et al. 2016). For both the squirrel cage and double-fed unit, the reactive power Qwt can be obtained for the range between v_{in} and v_{n} from (27).

3 Interval Power Flow

The IPF is used in the proposed methodology to solve the interval power flow Eqs. (9) and (10) and to give all interval variables previously defined. The IPF can measure the impact of uncertainties over load and generation on the system state, given by the nodal voltage magnitudes and phase angles, and on output variables as losses, currents and power from substation. IPF starts from the convergence of the deterministic power flow that is solved by using the Newton's method (Tinney and Hart 1967) to obtain the deterministic variables. The interval model is based on the Krawczyk's approach, an efficient technique for solving nonlinear interval systems that stems from the Newton's method (Oliveira et al. 2016; Pereira et al. 2012). The authors applied the sparse matrix inverse method known as QR decomposition (Ma et al. 2011; Huang and Tsai 2011) for treating the Jacobian matrix of the deterministic stage. The Newton's method was chosen since this method combined with interval-based analysis is consolidated in the literature (Wang and Alvarado 1992; Oliveira et al. 2016; Pereira et al. 2012). Notice that in the interval-based Newton's method (Krawczyk's approach), there is no need for inverting the Jacobian matrix, since this approach requires only multiplication of matrices, according to Wang and Alvarado (1992), Oliveira et al. (2016) and

Pereira et al. (2012), i.e., in the interval stage, there is no need for inverting the Jacobian matrix. The IPF steps are described hereafter (Oliveira et al. 2016).

Step 1 The state and output variables calculated through the deterministic power flow are used to obtain the corresponding interval variables.

Step 2 The variation percent of the load demand and wind-based DG is obtained from (11) to (14).

Step 3 The interval power mismatches of a bus f are calculated from (28) to (30). For a substation bus, $\Delta P_f^i = \Delta Q_f^i = 0$. In (30), $f(x)$ is the interval power mismatch vector and x is the state vector.

$$\Delta P_f^i = P_f^i - \left(Pwt_f^i - Pd_f^i\right), \tag{28}$$

$$\Delta Q_f^i = Q_f^i - \left(Qwt_f^i - Qd_f^i\right), \tag{29}$$

$$f(x) = \left[\Delta P^i \; \Delta Q^i\right]^t. \tag{30}$$

Step 4 The interval voltages are initialized according to (31)–(33) (Pereira and Costa 2014).

$$\begin{bmatrix} \Delta\theta^i \\ \Delta V^i \end{bmatrix} = \left(\mathrm{Jac}^d\right)^{-1} \begin{bmatrix} \Delta P^i \\ \Delta Q^i \end{bmatrix}, \tag{31}$$

$$\theta_f^i = \theta_f^d + \Delta\theta_f^i, \tag{32}$$

$$V_f^i = V_f^d + \Delta V_f^i. \tag{33}$$

Step 5 The Krawczyk operator, $K(x^h,X^h)$ consists of an interval set derived from an incremental value from x at iteration $h(x^h)$ that is calculated according to (34) (Oliveira et al. 2016; Pereira et al. 2012).

$$K\left(x^h, X^h\right) = x^h - C \cdot f\left(x^h\right) + \left(Id - C \cdot \mathrm{Jac}^i\left(X^h\right)\right) \cdot \left(X^h - x^h\right). \tag{34}$$

Step 6 The interval voltages are updated through the intersection of two interval sets as in (35) (Oliveira et al. 2016; Pereira et al. 2012). After that, the convergence criterion is checked by evaluating the difference $\left|r_X^{h+1} - r_X^h\right|$, where r_X is the radius of interval $X=[x_1;x_2]$ and is given by (36). If the largest difference among the interval variables is smaller than a pre-specified tolerance, ε^i, then the algorithm stops; otherwise, it returns to Step 5.

$$X^{h+1} = X^h \cap K\left(x^h, X^h\right), \tag{35}$$

$$r_X = \left(x_2 - x_1\right)/2. \tag{36}$$

Step 7 Any interval output variable (OV^i) can be calculated from the respective deterministic value (OV^d) and interval increment (ΔOV^i) from (37) (Oliveira et al. 2016; Pereira et al. 2012). The output variable function is linearized around the deterministic solution point by using Taylor series (Oliveira et al. 2016; Pereira et al. 2012), from (38) for a system with two buses, f and j, which allows obtaining the increment from the power mismatches according to (38).

$$OV^i = OV^d + \Delta OV^i, \tag{37}$$

$$\Delta OV^i = \left[\frac{\partial OV^d}{\partial \theta_f} X_P + \frac{\partial OV^d}{\partial V_f} Z_P + \frac{\partial OV^d}{\partial \theta_j} Y_P + \frac{\partial OV^d}{\partial V_j} W_P\right] \left[\Delta P^i \; \Delta Q^i\right]^t. \tag{38}$$

In this paper, the interval output variables OV^i comprise the currents in the EDS branches, the power supplied by substations and the power loss. Due to the dependence on the powers supplied by the substations, power loss and wind generation, the objective function to be minimized is given in interval form, according to (1). During the optimization process, the smallest interval objective function is obtained by a methodology for comparing intervals (Alolyan 2011) that uses a measure function μ, which is defined from the midpoint (m_x) and the radius (r_x) of an interval $X=[x_1;x_2]=\{x^* \in \mathrm{R} / x_1 \le x^* \le x_2\}$. The interval X can be defined as $X=(m_x,r_x)$ (Pereira et al. 2012; Alolyan 2011).

4 Proposed Algorithm

The proposed I-DSP algorithm combines the IPF method and the CLONR optimization algorithm (Oliveira et al. 2014) to handle the decision variables of constraints (23). The CLONR algorithm is based on the fundamentals of the metaheuristic AIS (Castro and Zuben 2002), and its steps can be found in Oliveira et al. (2014) and Oliveira et al. (2016). The basic structure of the I-DSP algorithm is presented by the flowchart of Fig. 1.

Stage-1 In Stage-1, the system data are read and the percent load variations, α_{pkl}, α_{pku}, α_{qkl} and α_{qku}, and percent wind speed variations, α_{wl} and α_{wu}, are set.

Stage-2 From the uncertainty degrees of Stage-1, the loads and the wind generation intervals can be obtained according to (11), (12) and (24)–(26), respectively.

Stage-3 It is performed at the first iteration of CLONR and gives the initial candidate solutions set P. Each element of P is an antibody that represents a candidate solution to the DSP problem. The repertoire P contains Nab antibodies, where each defines the decision binary variables of the problem $x_{fj,a}^{bc}, x_{fj,a}^{br}, x_f^{wt}, x_n^{sr}, x_n^{sc}, x_n^{oc}$ and x_{fj}^{cc}. The structure coding of each antibody is shown in Fig. 2. Part I determines the

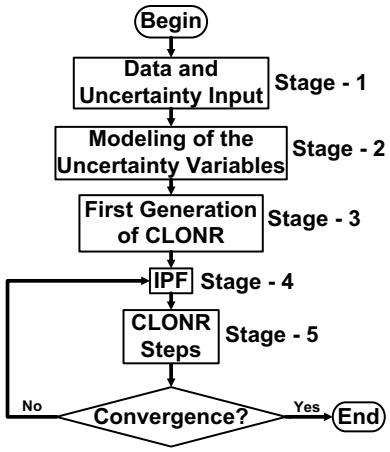

Fig. 1 Flowchart of the I-DSP algorithm

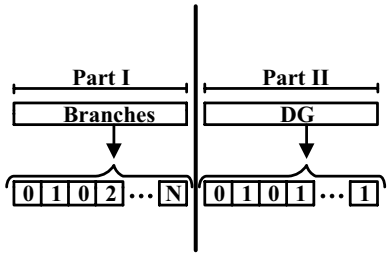

Fig. 2 Antibody coding

operating state of branches, where '0' indicates unbuilt branch and '*N*' indicates branch constructed with cable type *N*, which can be any positive integer real number. For an existing branch, a different type from the corresponding original one means a retrofit decision. Part II indicates a binary to determine which candidate buses are selected to install a wind turbine, where value '1' in *i*th position indicates wind turbine at *i*th candidate bus.

Notice that in the proposed codification, the substations selected to be built are automatically defined in Part I of the antibody. In this sense, if a candidate point for a new substation is connected to the network through the branches of Part I, then the corresponding substation is indicated as built. Moreover, the power supplied by the new and existing substations is determined by the IPF solution. If the power from a new substation is different from the empty interval, then the substation is built. In addition, an interval power from an existing substation greater than its deterministic nominal capacity means leads to an expansion decision. The comparisons between interval variables as well as between interval and deterministic ones are made by the interval comparison approach, where a deterministic variable can be represented by an interval with mean equal to the deterministic value and radius equal to zero. The antibodies represent only radial and connected topologies. For that, from the fully meshed network, a sequential opening of branches is done until constraint (22) is met. With the help of graph theory (Shin et al. 2007), no bus in the network is disconnected from the sequential opening of branches. Different radial and connected topologies are generated through the same procedure to form the initial set *P*.

Stage-4 The fitness of each candidate solution of *P* is evaluated as the inverse of the interval objective function of (1) obtained from the IPF solution. If a candidate solution violates any of the constraints (9)–(23), the objective function corresponding value will be penalized by a very high interval, reducing its evolution probability.

Stage-5 This stage comprises the CLONR evolutionary steps, which are described hereafter:

Step 1: Selection of the best candidate solutions for cloning—The best *nb* candidates of *P*, which presents the largest fitness values, are selected for cloning (Oliveira et al. 2014) through the interval comparison approach (Alolyan 2011).

Step 2: Cloning process—The number of clones for a selected candidate solution *i*, $N_C(i)$, is proportional to its normalized fitness as in (39) and $f^*(i)$ is the normalized fitness of candidate solution *i*, which are calculated according to (40) (Oliveira et al. 2014):

$$N_C(i) = round(\beta \cdot f^*(i)), \tag{39}$$

$$f^*(i) = 1/\left\{1 + e^{\left[-\left(\frac{f(i)-f_{av}}{\delta^*}\right)\right]}\right\}. \tag{40}$$

As the objective function and consequently the candidate solutions fitness are represented in interval forms, $f(i)$ is the midpoint fitness of *i*.

Step 3: Somatic hypermutation—Clone set solutions pass through the somatic hypermutation process that consists of a few modifications which are made in some clone candidate solutions according to a probability (Oliveira et al. 2014) by changing one of the decision variables of the antibody of Fig. 2. The mutation probability is inversely proportional to the clone normalized fitness from (41) (Oliveira et al. 2014).

$$p(ic) = e^{(-h \cdot f^*(ic))}. \tag{41}$$

A random value is generated for each clone, which is mutated if the value is lower than $p(ic)$. Otherwise, clone *ic* keeps unaltered. Notice that the mutation probabilities increase by reducing *h*, which is used to combine high and low mutation rates during the iterative process for improving the efficiency of the algorithm. The resulting mutant candidates are evaluated and the best *nb* are selected to replace the *n* worst ones of *P*.

Table 1 Parameters of CLONR and case study data

Nab	2**NBT*	*gimp*	5
gmax	120	*limd*	50%
β	20	ε^i	10^{-4}
nb	70%**Nab*	φ_S, φ_l	0.35
db	3%**Nab*	τ	10%
h	$h_1 = 1.0$, $h_2 = 0.2$	*T*	20 years
gest	20		

Step 4: *Receptor editing*—In this step, *db* candidates are randomly generated and replace the *db* worst ones of *P* to avoid the premature convergence at suboptimal solutions.

After *Step 4* in Stage 5, a generation is accounted and the convergence criterion is checked, which is achieved when the maximum number of iterations, *gmax*, is reached or when the best solution of *P* remains unchanged over *gest* iterations. Therefore, *gmax* and *gest* are parameters of the algorithm. If the convergence is not achieved, then the algorithm returns to Stage-4.

Table 1 presents the algorithm empirical parameters with some case study data. The high mutation started when the process stagnates over *gimp* iterations or when the solutions diversity reaches an inferior limit *limd* (Oliveira et al. 2014). The diversity of antibodies population (*div*) is calculated according to (42). More details can be found in Oliveira et al. (2014) and Oliveira et al. (2016).

$$div = Nab\_dist/Nab. \tag{42}$$

Tests to calibrate the previous CLONR parameters of the proposed algorithm were carried out, and those in Table 1 lead to the best planning results from exhaustive tests. These parameters were the same for all test systems in the manuscript.

5 Case Studies

Five test systems are used to evaluate the proposed I-DSP approach, since they are the more investigated in the literature for this problem, as the 9-bus (Falaghi et al. 2011), 23-bus (Lavorato et al. 2010; Nahman and Peric 2008; Gómez et al. 2004), 24-bus (Ortiz et al. 2018), 54-bus (Lavorato et al. 2010; Miranda et al. 1994), and the practical 136-bus system (Lavorato et al. 2010). The proposed approach is compared with deterministic methods (Lavorato et al. 2010; Nahman and Peric 2008; Gómez et al. 2004) to evaluate the impact of representing uncertainties over load and wind power-based DG, as well as with another uncertainty modeling method (Ortiz et al. 2018) to assess the efficacy of I-DSP. A constructive heuristic is applied in Lavorato et al. (2010), other metaheuristics in Nahman and Peric (2008) and Gómez et al. (2004) and a stochastic scenario-based approach that combines the strength of Tabu search algorithm and an efficient commercial optimization solver in Ortiz et al. (2018).

For comparison with the deterministic methods, a solution is obtained by the proposed algorithm with replacing the IPF of Stage-4 (Fig. 1) by a deterministic power flow that considers the function of (1) as deterministic. Therefore, the notation is:

1. Interval CLONR (ICLONR)—CLONR with the IPF embedded that seeks to minimize the objective function of (1) in its interval form, as proposed in this work;
2. Deterministic CLONR (DCLONR)—CLONR with a deterministic power flow embedded that minimizes the function of (1) in its deterministic form only for comparison. The interval cost of (1) is also calculated through the IPF for solutions from deterministic methods, including DCLONR, to evaluate the proposed interval method in minimizing its cost.

The solution from Ortiz et al. (2018), which also models uncertainties, is also evaluated through the IPF algorithm to be compared with the I-DSP. For a proper comparison, the same uncertainties levels in load and wind generation of Ortiz et al. (2018) are considered in the I-DSP approach. The interval loads are given by asymmetric variations, that is, the percent variations from the nominal load at a bus to its lower and upper limits are different from one another. Moreover, the variations are different between buses and the active variations are independent from the reactive ones. According to Zhang et al. (2012), such behavior fits the EDS features and, in this way, the analyses become more realistic (Ravadanegh et al. 2016; Pereira and Costa 2014). The samples of wind powers and speeds for squirrel cage units are given in Table 2, with inductive reactive powers. The active powers are also valid for double-fed units that have constant power factor. From Table 2, the power intervals of one wind unit are within [100;700] kW and [−200;−30] kVAr. The wind power features of Table 2 are used in all case studies, except for the 24-bus system, for which the same load and generation conditions of Ortiz et al. (2018) are considered for the proper comparison.

Table 2 Wind generators data

v (m/s)	*Pwt* (kW)	*Qwt* (kVAr)	*v* (m/s)	*Pwt* (kW)	*Qwt* (kVAr)
4.73	100	−30	8.85	400	−92
5.83	100	−30	9.73	500	−125
6.57	200	−40	11.14	600	−145
8.12	300	−60	11.69	700	−200

Table 3 Cable data, 9-bus

Type	Current capacity (A)	Resistance (Ω/km)	Reactance (Ω/km)	Cost (US$/km)
1	650	0.1738	0.2819	100,000.00
2	740	0.0695	0.2349	150,000.00

Table 4 Cable data, 23-bus

Type	Current capacity (A)	Resistance (Ω/km)	Reactance (Ω/km)	Cost (US$/km)
1	230	0.6045	0.4290	10,000.00
2	340	0.3017	0.4020	20,000.00

Table 5 Cable data, 24-bus

Type	Current capacity (A)	Resistance (Ω/km)	Reactance (Ω/km)	Cost (US$/km)
1	197	0.6140	0.3990	15,020.00
2	314	0.4070	0.3800	25,030.00

Table 6 Cable data, 54-bus

Type	Current capacity (A)	Resistance (Ω/km)	Reactance (Ω/km)	Cost (US$/km)
1	90	6.6607	4.5936	4000.00
2	110	5.3228	4.4940	7000.00

In the cases involving planning of wind power-based DG, 9-bus and 24-bus systems, the DG is considered as being owned by distribution companies and then it makes sense to select the best locations for adding DG. On the other hand, the case with the 54-bus system considers DG as owned by customers and then its place is fixed on their connecting buses. The 23-bus and 136-bus cases, in turn, do not consider DG in their networks. The cable types for the 9-bus (Falaghi et al. 2011), 23-bus (Lavorato et al. 2010; Nahman and Peric 2008; Gómez et al. 2004), 24-bus (Ortiz et al. 2018), 54-bus (Lavorato et al. 2010; Miranda et al. 1994) and 136-bus (Lavorato et al. 2010) system are given in Tables 3, 4, 5, 6 and 7, respectively.

In order to evaluate the IPF, a comparison analysis is made with Monte Carlo simulation (MCS), only for the final solution obtained by the ICLONR. For that, MCS considers load demand and wind speed as random variables according

Table 7 Cable data, 136-bus

Type	Current capacity (A)	Resistance (Ω/km)	Reactance (Ω/km)	Cost (US$/km)
1	600	0.8068	0.7038	4000.00

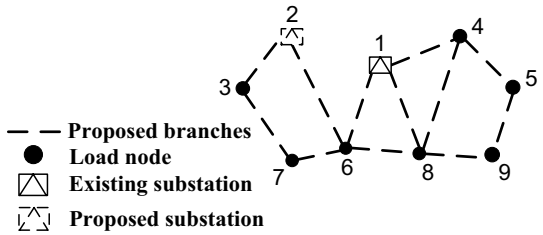

Fig. 3 The 9-bus test system

to each test, with 2,000,000 samples in each case study. For each test case, considering the evolutionary and probabilistic nature of the proposed algorithm, ten executions of ICLONR were performed and the same solution was obtained for each one. The algorithm was developed by using MATLAB@ version 8.10.0 (R2013a) and its interval mathematics toolbox INTLAB. The function polyfit was used to obtain the coefficients of (25) and (26) through polynomial regression (Valentine and Van Dine 1963). The tests were done by using an Intel® Core™ i7 CPU, 2.93 GHz, 16 GB RAM memory.

5.1 9-Bus System

This case study is used as a tutorial description to easy the understanding of the proposed approach. The 9-bus distribution test system illustrated in Fig. 3 is a 33 kV network composed of one existing substation at node '1' that cannot be expanded, one new proposed substation for bus '2' and 12 proposed branches represented by dotted lines. The maximum capacity of the substations is 20 MVA. The building cost of the proposed substation, CB, is US$ 1,000,000.00, the operation cost of DG, C_{wg}, is 0.04 US$/kWh, the price per purchase of energy in market, C_{pe}, is 0.01 US$/kWh and the substations operation cost, C_{op}, is 1e−06 US$/kVA^2 h. The voltage limits are given by a variation of 10%, the average power factor is 0.85 and the unit cost for energy loss, C_{l}, is 0.05 US$/kWh. The 9-bus system data can be found in Falaghi et al. (2011).

For the proposed IPF, the load variations percent is limited to 60% around their nominal values and random variations are chosen within this range for each bus. This limit is used because it impacts on the DSP problem, noting that it is even lower than the variations from Zhang et al. (2012). Two wind farms with eight squirrel cage wind generators units

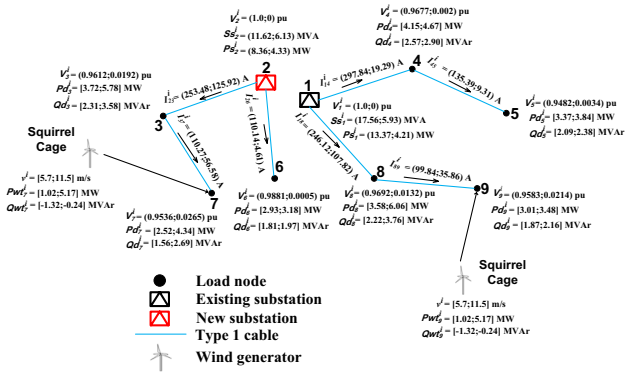

Fig. 4 Solution from ICLONR, 9-bus

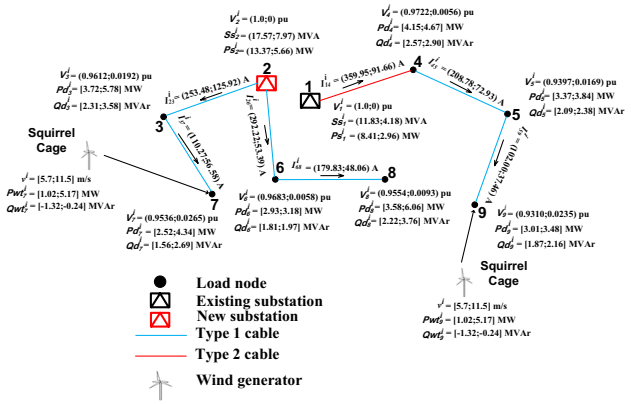

Fig. 5 Solution from DCLONR, 9-bus

can be installed, one at any of the candidate buses 3, 4, 7, 8 and 9. The installation cost of a wind farm, *CWT*, is US$ 100,000.00. The penetration of wind power was defined to impact the DSP problem and is below the limit of 30% of the system load (Naderi et al. 2012; Porkar et al. 2010; Oliveira et al. 2016). The IPF considers an asymmetric variation around the speed value 6.0 m/s with the range [5.7;11.5] m/s. The DCLONR used for comparison considers the fixed load of Falaghi et al. (2011) and the wind speed at 6.0 m/s.

Figures 4 and 5 show the topologies and the interested IPF variables from the proposed ICLONR and from the DCLONR, respectively, where the interval input variables *Pd*, *Qd*, *v*, *Pwt* and *Qwt* are given in the form [min. value;max.value] and the output interval variables *V*, *I*, *Ps* and *Ss* are in the form (midpoint;radius) to easy the comparisons. Table 8 presents the results from ICLONR and DCLONR, where the notation for any interval cost is given by a pair (midpoint;radius), obtained through the IPF. Table 9 gives the results from MCS.

The proposed ICLONR determines a plan different from the deterministic version. The total cost midpoint and radius from the proposed interval solution are lower than the respective values from the deterministic, with an average saving of US$ 270,000.00 or 0.45%, showing that uncertainties over the load and wind generation impact on the DSP and must be considered. The MCS supports that the proposed interval solution provides lower m_x and r_x for the objective function to be minimized in comparison with deterministic. Figure 6 presents the evolution of the total cost midpoint and radius over the ICLONR iterations to show the convergence of the proposed algorithm, which converges to the smallest values found along the optimization process.

5.2 23-Bus System

This system has the data available in Lavorato et al. (2010), Nahman and Peric (2008) and Gómez et al. (2004). The cables of Table 4 are considered for expansion and the existing substation cannot be expanded. The voltage limits are given by 3% around the nominal value, the average inductive power factor is 0.90 and the energy loss cost is 0.05 US$/kWh. For the proposed interval approach, the load variations

Table 8 Results (MUS$), 9-bus

Solutions	Branch cost	Loss cost	Substation and DG cost	Operational cost of substation and DG	Energy purchase cost	Total cost
ICLONR	9.2	(0.77;0.47)	1.2	(31.93;21.53)	(16.21;6.37)	(59.31;28.37)
DCLONR	9.0	(0.84;0.56)	1.2	(32.30;22.28)	(16.24;6.43)	(59.58;29.27)

Table 9 Results from MCS (MUS$), 9-bus

Solutions	Branch cost	Loss cost	Substation and DG cost	Operational cost of substation and DG	Energy purchase cost	Total cost
ICLONR	9.2	(0.76;0.44)	1.2	(31.43;20.87)	(15.81;5.82)	(58.40;27.13)
DCLONR	9.0	(0.81;0.55)	1.2	(31.80;21.62)	(15.84;5.88)	(58.65;28.05)

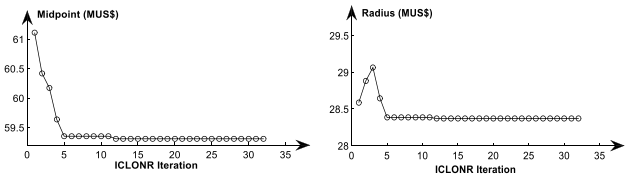

Fig. 6 Evolution of the total cost midpoint and radius, 9-bus

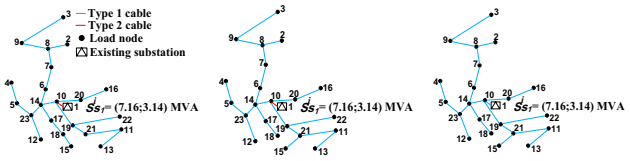

(a) ICLONR **(b)** DCLONR **(c)** Lavorato et al. (2010); Nahman and Peric (2008); Gómez et al. (2004)

Fig. 7 Solutions, 23-bus *Test* 1

are limited to 65% and the same procedure of the previous case is used to generate the load intervals. The deterministic simulation through the DCLONR considers the fixed load of Lavorato et al. (2010), Nahman and Peric (2008) and Gómez et al. (2004) whose results are also used for comparison. Two tests are performed: *Test* 1—planning considering only one existing substation; *Test* 2—planning considering also a candidate substation. In both tests, there are no DG units, and the investment cost in DG and the cost of purchase energy are not considered for fitting the models presented in other works for proper comparison.

(1) *Test* 1—The maximum capacity of substation at node '1' is 10 MVA and its operation cost is not considered for comparison with other works. Figure 7 shows the topologies from the proposed interval solution, the deterministic DCLONR and Lavorato et al. (2010), Nahman and Peric (2008) and Gómez et al. (2004), with the costs given in Table 10.

It can be observed that the proposed interval approach determines a topology different from the deterministic solutions, with the lowest total cost midpoint and average saving of 0.17% related to DCLONR. Despite the larger radius of ICLONR for this case, its interval cost is the lowest according to the interval comparison approach of Alolyan (2011). It is also noteworthy that the DCLONR solution is better than the solutions from Lavorato et al. (2010), Nahman and Peric (2008), Gómez et al. (2004), in terms of the interval total cost. This result shows the efficiency of the AIS technique.

(2) *Test* 2—In this test, the maximum capacity of the existing substation at node '1' is 4 MVA, and another substation of 4 MVA can be built at node '2' with a cost of US$ 1,000,000.00. The operation cost for both substations is 1e−05 US$/kVA^2 h. In such condition, the DCLONR solution is equal to that from Lavorato et al. (2010), Nahman and Peric (2008) and Gómez et al. (2004). Figure 8 shows the topologies obtained by the interval proposed approach and the deterministic solution, whose intervals from IPF are given in Table 11. Note that the interval apparent power from substation at bus '1' exceeds the limit of (20), according to the interval comparison approach of Alolyan (2011), for the deterministic solution when evaluated considering the load uncertainty. It does not occur for the topology obtained by using the proposed ICLONR. Moreover, the ICLONR gives the lowest total cost midpoint and radius with an average saving of 4.56% related to DCLONR and Lavorato et al. (2010), Nahman and Peric (2008) and Gómez et al. (2004).

5.3 54-Bus System

The 54-bus distribution test system is a 13.5 kV network whose data can be found in Lavorato et al. (2010) and Miranda et al. (1994). The cables of Table 6 are considered for expansion, and there are four substations, S1–S4, where S1 and S2 are existent and can be expanded and S3 and S4 are new proposed substations (Lavorato et al. 2010; Miranda et al. 1994). The capacity of S1 and S2 is 0.167 MVA, S1 can add 0.167 MVA at US$ 100,000.00 and S2 can

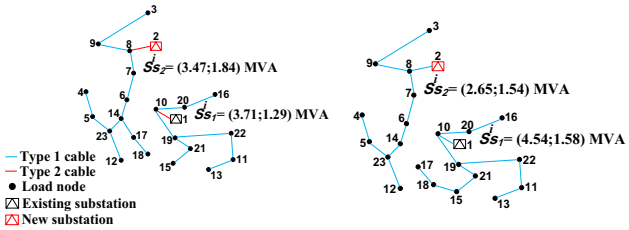

(a) ICLONR **(b)** DCLONR

Fig. 8 Solutions, 23-bus *Test* 2

Table 10 Results (US$), 23-bus *Test* 1

Solutions	Branch cost	Loss cost	Total cost
ICLONR	153,913	(13,784;11,296)	(167,700;11,300)
DCLONR	154,271	(13,718;11,130)	(167,985;11,135)
Lavorato et al. (2010), Nahman and Peric (2008), Gómez et al. (2004)	151,892	(16,942;13,674)	(168,835;13,675)

Table 11 Results, 23-bus *Test* 2

Solutions	Branch cost (US$)	Loss cost (US$)	Substation cost (MUS$)	Operational cost (MUS$)	Total cost (MUS$)
ICLONR	151,260	(13,476;10,609)	1.00	(8.04;5.82)	(9.20;5.83)
DCLONR	149,712	(13,954;10,196)	1.00	(8.47;5.87)	(9.64;5.88)

Table 12 Results, 54-bus *Test* 1

Solutions	Branch cost (US$)	Loss cost (US$)	Substation cost (US$)	Operational cost (MUS$)	Total cost (MUS$)
ICLONR	39,452	(2429.70;1616.30)	540,000	(2.51;1.64)	(3.10;1.65)
DCLONR, Lavorato et al. (2010)	39,576	(2054.25;1371.75)	540,000	(2.57;1.61)	(3.15;1.61)

add 0.133 MVA at US$ 80,000.00. S3 and S4 can be built with a capacity of 0.222 MVA at US$ 200,000.00 and US$ 240,000.00, respectively. The cost for retrofitting type '1' cables of existing branches by type '2' cables, CR_{12}, is given by the difference between their respective costs (Lavorato et al. 2010; Miranda et al. 1994). Two tests are performed: *Test* 1—planning without considering the installation of DG; *Test* 2—planning considering the presence of DG at predetermined customer's buses. In both tests, the investment and operation costs of the DGs are not considered, as well as the cost of purchase energy in market to fit the models proposed in other works for comparison.

Test 1 considers a 5% variation for voltages, average power factor 0.92, energy loss cost 0.10 US$/kWh, substations operation cost 1e−03 US$/kVA^2 h, load variations limited to 60% and fixed load of deterministic solution from Lavorato et al. (2010) and Miranda et al. (1994). Table 12 presents the costs through IPF, where the proposed interval differs from the other with an average saving of US$ 50,000.00. The proposed method leads to the lowest cost midpoint and smaller interval according to Alolyan (2011).

In *Test* 2, two equal double-fed wind generators are placed at buses 4 and 13 with unit power factors. The wind powers' data of Table 2 are divided by two to better fit to this system, leading to the values of Table 13. The wind speed of the deterministic solution is 5.3 m/s, and the interval approach considers an asymmetric variation within [5;11] m/s. The other conditions are the same of *Test* 1. Table 14 presents the costs from IPF, where the proposed ICLONR provides the smallest total cost midpoint and radius with an average saving of US$ 160,000.00 in relation to the deterministic topology. The saving of *Test* 2 is larger than that of *Test* 1, which shows that the representation of more uncertainties such as the wind generation impacts more on the DSP and, therefore, should be done.

Table 13 Wind generators data, 54-bus

v (m/s)	Pwt (kW)	Qwt (kVAr)	v (m/s)	Pwt (kW)	Qwt (kVAr)
4.73	50	−15	8.85	200	−46
5.83	50	−15	9.73	250	−62.5
6.57	100	−20	11.14	300	−72.5
8.12	150	−30	11.69	350	−100

5.4 136-Bus System

The practical 136-bus distribution test system is a 13.8 kV network whose data can be found in Lavorato et al. (2010). The cable of Table 7 is considered for expansion, and there are two substations of 15 MVA and 10 MVA. The planning option is to transfer loads between the substations through investment in branches and reconfiguration. The cost for opening an existing switch is not considered. The allowed voltage variation is 7%, the average power factor is 0.92 and the energy loss and substations operation costs are 0.001US$/kWh and 1e−06US$/kVA^2 h, respectively. The system has no DG and the purchase energy cost is not considered to fit the model proposed in Lavorato et al. (2010), which is used for comparison. The load variations are limited to 60%, and the deterministic solution considers the fixed load of Lavorato et al. (2010). The main planning data can be found in Lavorato et al. (2010). Table 15 presents the costs from IPF, where ICLONR gives the smallest (midpoint;radius) for total cost.

5.5 24-Bus System

The 24-bus system of Ortiz et al. (2018) is used to show the performance of the proposed I-DSP approach in comparison with another method that also considers uncertainties for the DSP, i.e., the stochastic scenario-based approach presented in Ortiz et al. (2018).

Table 14 Results, 54-bus *Test* 2

Solutions	Branch cost (US$)	Loss cost (US$)	Substation cost (US$)	Operational cost (MUS$)	Total cost (MUS$)
ICLONR	39,952	(2281.11;1498.03)	440,000	(2.87;2.63)	(3.35;2.63)
DCLONR	39,452	(2407.05;1884.99)	440,000	(3.03;2.65)	(3.51;2.65)

Table 15 Results, 136-bus

Solutions	Branch cost (US$)	Loss cost (US$)	Operational cost (MUS$)	Total cost (MUS$)
ICLONR	4360	(11,550;8348.5)	(6.42;4.61)	(6.44;4.62)
DCLONR	4000	(12,873;9018)	(6.68;4.71)	(6.70;4.72)
Lavorato et al. (2010)	5360	(13,022;9124.5)	(6.73;4.74)	(6.75;4.75)

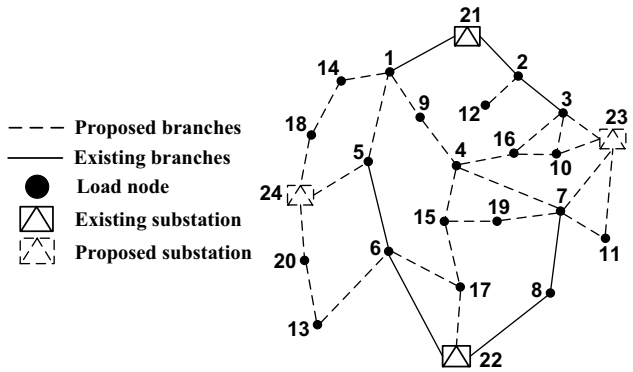

Fig. 9 The 24-bus test system

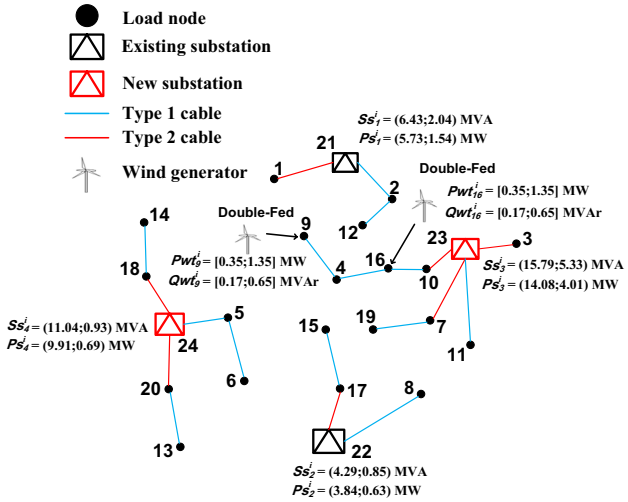

Fig. 10 Solution from ICLONR and Ortiz et al. (2018), 24-bus

The system consists of 20 load buses with a constant power behavior, four substations operating at 20 kV and 34 branches where 27 are candidate branches and seven are existing branches that can be reconfigured. The cables of Table 5 are considered for expansion. Only two double-fed wind generators with capacity 3 MVA and installation cost, *CWT*, US$ 100,000.00 can be installed in the system. The parameters of the wind turbine are $v_{in} = 3.5$ m/s, $v_n = 15$ m/s and $v_{ou} = 25$ m/s. Buses 5, 9, 15 and 16 are candidates to install a wind turbine.

The planning horizon is 15 years. The upper and lower voltage limits are 1.00 and 0.95 pu, respectively. The energy price is 0.1 US$/kWh, the operation cost of DG is 0.04 US$/kWh, the lagging power factor for the system is 0.9 and the leading power factor for DGs is 0.9. In this case study, the costs of energy loss and substation operating are not considered to have the same objective function proposed in Ortiz et al. (2018). The system before planning is illustrated in Fig. 9. In the initial system, buses 21 and 22 are existent substations that can be expanded, and buses 23 and 24 are new proposed places for substations. The capacity of buses 21 and 22 is 7 and 5 MVA, respectively, and they can add 14 MVA at US$ 120,000.00 and 10 MVA at US$ 115,000.00, respectively. At buses 23 and 24, substations can be built with a capacity of 17 MVA at US$ 380,310.00 and 15 MVA at US$ 280,260.00, respectively. The cost for retrofitting type '1' cables of existing branches by type '2' cables, CR_{12}, is given by US$ 19,140.00.

The load variations are limited to 50%, and this uncertainty level is the same used in the scenarios proposed in Ortiz et al. (2018). The active and reactive powers dispatched by the wind generators are comprised of the intervals [0.35;1.35] MW and [0.17;0.65] MVAr, respectively, which also present the same uncertainty levels practiced in the scenarios of Ortiz et al. (2018). The solutions proposed by the interval approach and the scenario-based technique from Ortiz et al. (2018) are topologically the same as shown in Fig. 10, with the costs given in Table 16.

Therefore, the ICLONR solution can provide the same expansion plan as the in Ortiz et al. (2018) solution with a more computational efficiency, since ICLONR solution requires a time of 20 min while the solution of Ortiz et al.

Table 16 Results (MUS$), 24-bus

Solutions	Branch cost	Substation and DG cost	Operational cost of DG	Energy purchase cost	Total cost
ICLONR	0.70	0.86	(4.53;2.67)	(223.62;45.83)	(229.72;48.50)
Ortiz et al. (2018)	0.70	0.86	(4.53;2.67)	(223.62;45.83)	(229.72;48.50)

(2018) spends 90 min. This is due to the fact that, in the proposed interval approach, all uncertainties scenarios of load and wind generation are represented and evaluated in a single step and their impacts on the objective function are measured through the interval mathematics fundamentals. On the other hand, the stochastic scenario-based approach of Ortiz et al. (2018) spends more computational time because it requires the calculation of a new deterministic load flow for each scenario.

The maximum relative percent errors between IPF and MCS are given in Table 17 for all tests and case studies with the average processing times of ten simulations of the ICLONR algorithm for each test. Although there are some errors between the IPF and MCS intervals, the MCS supports that the interval proposed approach gives the smallest total interval costs in all tests. Notice that although some processing times of Table 17 can be considered relatively large, the problem handled in the present paper is a long-term planning problem, which does not require very small processing times. In other words, the processing time, since being not prohibitive for the planning analyses, is not a key issue (Bagheri et al. 2015; Ortiz et al. 2019; Munoz-Delgado et al. 2016). For instance, references (Ortiz et al. 2018, 2019; Munoz-Delgado et al. 2016) find optimal solutions for the planning problem of test systems 24, 54 and 136 within times greater than those respective times from Table 17. It can be highlighted that the time required by IPF is approximately 80,000 times lower than by MCS. This is because that for every final solution, the IPF is performed a unique time, i.e., this technique does not require several evaluations for a given solution considering the related uncertainties, unlike the MCS that must evaluate several samples for the random variables for each final solution.

6 Conclusions

This paper proposed an interval optimization approach to solve the power system distribution expansion planning that considers uncertainties over loads and distributed generation based on wind power. An interval artificial immune system is proposed to minimize the investment and operation costs, subject to network and operational constraints. The uncertainties over the planning input variables are propagated to output ones through an interval power flow and used to evaluate candidate topologies in terms of their interval total costs. From the results, it can be concluded that:

- the representation of uncertainties has a significant impact on the DSP problem;
- the proposed methodology results in smaller interval cost related to solutions that do not consider uncertainties, according to an interval comparison;
- the proposed interval methodology found the same expansion plan of the stochastic scenario-based technique, another method for modeling uncertainties widely used in the literature, with a much lower computational effort; and
- the intervals from the IPF are compared with those from classical MCS, and the errors between them can validate the results with much less computational effort.

Therefore, the proposed approach presents a contribution for the literature through a novel method to model load and wind DG uncertainties in the DPS problem in a coupled manner. An interesting proposal for future work is the evaluation of more wind conversion technologies, such as synchronous generators or full converter. If focus is on induction

Table 17 Processing times and errors between IPF and MCS

Test	ε_{vo} (%)	ε_{cu} (%)	ε_{ap} (%)	ε_{acp} (%)	ε_{lo} (%)	ε_{op} (%)	ε_{pe} (%)	ε_{tc} (%)	Time (s)
9-Bus	0.35	3.2	6.57	5.85	7.69	2.22	4.39	2.51	500.40
23-Bus *Test* 1	0.04	5.74	9.55	8.43	9.29	NA	NA	1.43	1020.30
23-Bus *Test* 2	0.02	6.86	8.91	7.52	9.59	9.86	NA	9.19	1080.50
54-Bus *Test* 1	0.03	8.90	9.00	8.38	9.27	9.39	NA	9.53	1810.70
54-Bus *Test* 2	0.07	9.50	9.77	8.65	9.89	9.58	NA	9.26	2116.20
136-Bus	0.50	8.34	9.42	9.13	10.09	10.27	NA	10.21	4212.50
24-Bus	0.05	5.92	8.57	7.35	NA	1.63	5.18	5.73	1200.00

machines, it can be also a fully rated converter. The different technologies rule the reactive power limits and impact on interval power injections.

Acknowledgements The authors would like to thank the 'Coordination for the Improvement of Higher Education Personnel' (CAPES), 'Foundation for Supporting Research in Minas Gerais' (FAPEMIG), 'Brazilian National Research Council' (CNPq), 'Electric Power National Institute' (INERGE) and 'Heuristic and Bioinspired Optimization Group' (GOHB) for supporting this research.

References

Ahmadigorji, M., Amjady, N., & Dehghan, S. (2018). A robust model for multiyear distribution network reinforcement planning based on information-gap decision theory. *IEEE Transactions on Power Systems, 33*(2), 1339–1351.

Alishahi, E., Moghaddam, M. P., & Sheikh-El-Eslami, M. K. (2012). A system dynamics approach for investigating impacts of incentive mechanisms on wind power investment. *International Journal of Renewable Energy, 37*(1), 310–317.

Alolyan, I. (2011). A new method for comparing closed intervals. *Australian Journal of Mathematical Analysis and Applications, 8*(1), 1–6.

Amjady, N., Attarha, A., Dehghan, S., & Conejo, A. J. (2018). Adaptive robust expansion planning for a distribution network with DERs. *IEEE Transactions on Power Systems, 33*(2), 1698–1715.

Asensio, M., de Quevedo, P. M., Muñoz-Delgado, G., & Contreras, K. (2018). Joint distribution network and renewable energy expansion planning considering demand response and energy storage—Part I: Stochastic programming model. *IEEE Transactions on Smart Grid, 9*(2), 655–666.

Bagheri, A., Monsef, H., & Lesani, H. (2015). Integrated distribution network expansion planning incorporating distributed generation considering uncertainties, reliability, and operational conditions. *Electrical Power and Energy Systems, 73*(1), 56–70.

Bin Humayd, A. S., & Bhattacharya, K. (2017). Distribution system planning to accommodate distributed energy resources and PEVs. *International Journal of Electrical Power & Energy Systems, 145*(1), 1–11.

Borges, C. L. T., & Martins, V. F. (2012). Multistage expansion planning for active distribution networks under demand and distributed generation uncertainties. *International Journal of Electrical Power & Energy Systems, 36*(1), 107–116.

Castro, L. N., & Zuben, F. J. V. (2002). Learning and optimization using the clonal selection principle. *IEEE Transactions on Evolutionary Computation, 6*(3), 239–251.

Chaturvedi, A., Prasad, K., & Ranjan, R. (2006). Use of interval arithmetic to incorporate the uncertainty of load demand for radial distribution system analysis. *IEEE Transactions on Power Delivery, 21*(2), 1019–1021.

Ehsan, A., Cheng, M., & Yang, Q. (2019). Scenario-based planning of active distribution systems under uncertainties of renewable generation and electricity demand. *CSEE Journal of Power and Energy Systems, 5*(1), 56–62.

Falaghi, H., Singh, C., Haghifam, M. R., & Ramezani, M. (2011). DG integrated multistage distribution system expansion planning. *International Journal of Electrical Power & Energy Systems, 33*(8), 1489–1497.

Gómez, J. F., Khodr, H. M., Oliveira, P. M., Ocque, L., Yusta, J. M., Villasana, R., et al. (2004). Ant colony system algorithm for the planning of primary distribution circuits. *IEEE Transactions on Power Systems, 19*(2), 996–1004.

Huang, Z. Y., & Tsai, P. Y. (2011). Efficient implementation of QR decomposition for gigabit MIMO-OFDM systems. *IEEE Transactions on Circuits and Systems, 58*(10), 2531–2542.

Junior, B. R. P., Cossi, A. M., Contreras, J., & Mantovani, J. R. S. (2014). Multiobjective multistage distribution system planning using tabu search. *IET Generation, Transmission and Distribution, 8*(1), 35–45.

Lavorato, M., Rider, M. J., Garcia, A. V., & Romero, R. A. (2010). A constructive heuristic algorithm for distribution system planning. *IEEE Transactions on Power Systems, 25*(3), 1734–1742.

Ma, L., Dickson, K., McAllister, J., & McCanny, J. (2011). QR decomposition-based matrix inversion for high performance embedded MIMO receivers. *IEEE Transactions on Signal Processing, 59*(4), 1858–1867.

Mazhari, S. M., Monsef, H., & Romero, R. (2016). A multi-objective distribution system expansion planning incorporating customer choices on reliability. *IEEE Transactions on Power Systems, 31*(2), 1330–1340.

Miranda, V., Ranito, J. V., & Proença, L. M. (1994). Genetic algorithm in optimal multistage distribution network planning. *IEEE Transactions on Power Systems, 9*(4), 1927–1933.

Munoz-Delgado, G., Contreras, J., & Arroyo, J. M. (2016). Multistage generation and network expansion planning in distribution systems considering uncertainty and reliability. *IEEE Transactions on Power Systems, 31*(5), 3715–3728.

Naderi, E., Seifi, H., & Sepasian, M. S. (2012). A dynamics approach for distribution system planning considering distributed generation. *IEEE Transactions on Power Systems, 27*(3), 1313–1322.

Nahman, J. M., & Peric, D. M. (2008). Optimal planning of radial distribution networks by simulated annealing technique. *IEEE Transactions on Power Systems, 23*(2), 790–795.

Oliveira, L. W., Oliveira, E. J., Gomes, F. V., Silva Junior, I. C., Marcato, A. L. M., & Resende, P. V. C. (2014). Artificial immune systems applied to the reconfiguration of electrical power distribution networks for energy loss minimization. *International Journal of Electrical Power & Energy Systems, 56*(1), 64–74.

Oliveira, L. W., Seta, F. S., & Oliveira, E. J. (2016). Optimal reconfiguration of distribution systems with representation of uncertainties through interval analysis. *International Journal of Electrical Power & Energy Systems, 83*(1), 382–391.

Ortiz, J. M. H., Melgar-Dominguez, O. D., Pourakbari-Kasmaei, M., & Mantovani, J. R. S. (2019). A stochastic mixed-integer convex programming model for long-term distribution system expansion planning considering greenhouse gas emission mitigation. *Electrical Power and Energy Systems, 108*(1), 86–95.

Ortiz, J. M. H., Pourakbari-Kasmaei, M., López, J., & Mantovani, J. R. S. (2018). A stochastic mixed-integer conic programming model for distribution system expansion planning considering wind generation. *Energy Systems, 9*(33), 1–21.

Pereira, L. E. S., & Costa, V. M. (2014). Interval analysis applied to the maximum loading point of electric power systems considering load data uncertainties. *International Journal of Electrical Power & Energy Systems, 54*(1), 334–340.

Pereira, L. E. S., Costa, V. M., & Rosa, A. L. S. (2012). Interval arithmetic in current injection power flow analysis. *International Journal of Electrical Power & Energy Systems, 43*(1), 1106–1113.

Porkar, S., Poure, P., Abbaspour-Tehrani-Fard, A., & Saadate, S. (2010). A novel optimal distribution system planning framework implementing distributed generation in a deregulated electricity market. *International Journal of Electric Power Systems Research, 80*(7), 828–837.

Qiao, Z., Guo, Q., Sun, H., Pan, Z., Liu, Y., & Xiong, W. (2017). An interval gas flow analysis in natural gas and electricity coupled

networks considering the uncertainty of wind power. *Applied Energy, 201*(1), 343–353.

Rasmussen, T. B., Yang, G., & Nielsen, A. H. (2019). Interval estimation of voltage magnitude in radial distribution feeder with minimal data acquisition requirements. *Electrical Power and Energy Systems, 113*(1), 281–287.

Ravadanegh, S. N., Jahanyari, N., Amini, A., & Taghizadeghan, N. (2016). Smart distribution grid multistage expansion planning under load forecasting uncertainty. *IET Generation, Transmission and Distribution, 10*(5), 1136–1144.

Sahoo, N. C., & Ganguly, S. (2011). Simple heuristics-based selection of guides for multi-objective PSO application to electrical distribution system planning. *International Journal of Engineering Applications of Artificial Intelligence, 24*(4), 567–585.

Saric, A. T., & Stankovic, A. M. (2006). An application of interval analysis and optimization to electric energy markets. *IEEE Transactions on Power Systems, 21*(2), 515–523.

Shin, J. R., Kim, B. S., Park, J. B., & Lee, K. Y. (2007). A new optimal routing algorithm for loss minimization and voltage stability improvement in radial power system. *IEEE Transactions on Power Systems, 22*(2), 648–657.

Tinney, W. F., & Hart, C. E. (1967). Power flow solution by Newton's method. *IEEE Transactions on Power Apparatus and Systems, PAS-86*(11), 1449–1460.

Valentine, C. W., & Van Dine, C. P. (1963). An algorithm for minimax polynomial curve-fitting of discrete data. *The Journal of the Association for Computing Machinery (JACM), 10*(3), 283–290.

Vélez, V. M., Hincapíe, R. A., & Gallego, R. A. (2014). Low voltage distribution system planning using diversified demand curves. *International Journal of Electrical Power & Energy Systems, 61*(1), 691–700.

Wang, Z., & Alvarado, F. L. (1992). Interval arithmetic in power flow analysis. *IEEE Transactions on Power Systems, 7*(3), 1341–1349.

Zhang, S., Cheng, H., Wang, D., Zhang, L., Li, F., & Yao, L. (2018). Distributed generation planning in active distribution network considering demand side management and network reconfiguration. *Applied Energy, 228*(1), 1921–1936.

Zhang, P., Li, W., & Wang, S. (2012). Reliability-oriented distribution network reconfiguration considering uncertainties of data by interval analysis. *International Journal of Electrical Power & Energy Systems, 34*(1), 138–144.